J Therm Anal Calorim (2012) 107:1129–1135
DOI 10.1007/s10973-011-1535-4

Thermal studies of $ZnO–B_2O_3–P_2O_5–TeO_2$ glasses

P. Mošner · K. Vosejpková · L. Koudelka · L. Beneš

Received: 16 February 2011 / Accepted: 23 March 2011 / Published online: 8 April 2011

Abstract The effect of TeO_2 additions on the thermal behaviour of zinc borophosphate glasses were studied in the compositional series $(100 - x)[0.5ZnO–0.1B_2O_3–0.4P_2O_5]–xTeO_2$ by differential scanning calorimetry, thermodilatometry and heating microscopy thermal analysis. The addition of TeO_2 to the starting borophosphate glass resulted in a linear increase of glass transition temperature and dilatometric softening temperature, whereas the thermal expansion coefficient decreased. Most of glasses crystallize under heating within the temperature range of 440–640 °C. The crystallization temperature steeply decreases with increasing TeO_2 content. The lowest tendency towards crystallization was observed for the glasses containing 50 and 60 mol% TeO_2. X-ray diffraction analysis showed that major compounds formed by annealing of the glasses were $Zn_2P_2O_7$, BPO_4 and α-TeO_2. Annealing of the powdered $50ZnO–10B_2O_3–40P_2O_5$ glass leads at first to the formation of an unknown crystalline phase, which is gradually transformed to $Zn_2P_2O_7$ and BPO_4 during subsequent heating.

Keywords Borophosphate glasses · Tellurite glasses · Thermal properties · Thermal stability · Crystallization

P. Mošner (✉) · K. Vosejpková · L. Koudelka
Department of General and Inorganic Chemistry, Faculty of Chemical Technology, University of Pardubice, Studentská 573, 532 10 Pardubice, Czech Republic
e-mail: petr.mosner@upce.cz

L. Beneš
Faculty of Chemical Technology, Joint Laboratory of Solid State Chemistry of the Institute of Macromolecular Chemistry of Academy of Sciences, v.v.i., and University of Pardubice, Studentská 84, 532 10 Pardubice, Czech Republic

Introduction

It is known that both phosphate and borate glasses usually possess low chemical durability [1, 2] which is a very important feature for their practical applications. Simultaneously, it was found that the addition of B_2O_3 into the phosphate glasses or P_2O_5 into the borate glasses leads to improving of their chemical stability due to the formation of P–O–B linkages in the glass network [3–5]. The addition of B_2O_3 into the phosphate glasses improves also their mechanical [6] and optical properties [7] and leads to an increase of ionic conductivity [8] of phosphate glasses. Furthermore, the incorporation of boron oxide into the phosphate network initially reduced the tendency towards crystallization, but high B_2O_3 content leads to lower thermal stability of borophosphate glasses [9]. The progress in the studies of borophosphate glasses is manifested in the development of new glasses with unconventional properties and novel applications such as biomedical materials, sealing and packaging materials, solid electrolytes, etc. [4, 10, 11].

Recently, there was an increasing interest also in the study of zinc borophosphate glasses [12–16]. Glass-forming region in the $ZnO–B_2O_3–P_2O_5$ system was published by Ushakov et al. [12] and structure of zinc borophosphate glasses was described in papers [13–15]. The relations between structure and properties of glasses within $ZnO–B_2O_3–P_2O_5$ ternary system were published in [15], while kinetics and mechanism of crystallization of $ZnO–B_2O_3–P_2O_5$ glasses was studied in [16]. It was found that that the replacement of P_2O_5 by B_2O_3 leads to an increase of glass transition temperature and dilatation softening temperature, while the linear coefficient of thermal expansion decreases with increasing B_2O_3 content [15]. The analysis of the crystallization peak showed that for the borophosphate

glasses with high P_2O_5 content surface crystallization prevail; while for the glasses containing high B_2O_3 content internal crystallization prevail [16]. The crystallization takes place mostly at 600–800 °C giving crystalline BPO_4 and $Zn_2P_2O_7$ or $Zn(PO_3)_2$ compounds.

The doping of zinc borophosphate glasses with other network formers such as TeO_2, MoO_3 or WO_3 can offer an additional modification of their physical properties. Only a few papers were published on the glasses containing P_2O_5, B_2O_3 and TeO_2 [17–19], although addition of TeO_2 into the borophosphate glasses can bring a lot of useful properties including low melting temperature, high refractive indices, high transmission in the infrared region, high dielectric constant, etc., which could result in wide application in fibre optics and laser technology.

This paper is devoted to the $ZnO–B_2O_3–P_2O_5–TeO_2$ glasses with the ratio of $B_2O_3/P_2O_5 = 10/40$. The aim of this work is to study thermal properties of the compositional series of $(100 - x)[0.5ZnO–0.1B_2O_3–0.4P_2O_5]–xTeO_2$ glasses in a broad range of TeO_2 content.

Experimental

Glasses of the $ZnO–B_2O_3–P_2O_5–TeO_2$ system were prepared by conventional melt-quenching method using a total batch weight of 20 g. Stochiometric starting mixtures of analytical grade raw materials ZnO, TeO_2, H_3BO_3 and H_3PO_4 were slowly calcined up to 600 °C for 2 h to remove water. After the calcinations, the reaction mixtures were heated up to 900–1250 °C in a Pt crucible covered with a lid, followed by mixing and homogenization for 30 min. The melts were cooled by pouring into a graphite mould in air. Obtained glasses were annealed for 30 min at a temperature 5 °C below their glass transition temperature to improve their mechanical properties. The final products were stored over silica gel in a desiccator.

The thermal behaviour of glasses was studied with the DTA 404 PC (NETZSCH) operating in the DSC mode, horizontal pushrod dilatometer DIL 402PC (NETZSCH) and with heating microscope (Hesse Instruments). DSC measurements were carried out at the heating rate of 10 °C min^{-1} under a flowing atmosphere of N_2. Powder samples of glasses (100 mg) with a mean diameter $\sim$10 μm were placed in open silica crucibles. The empty silica crucible was used as a reference material. For these measurements, glassy samples were pulverized in a vibrational mill with the corundum lining. Dilatometric curves of the glasses were obtained on bulk samples with dimensions of $\sim 5 \times 5 \times 20$ mm at the heating rate of 5 °C min^{-1}. Samples were measured in static air atmosphere using sample holder from Al_2O_3, between two alumina plates subjected to compressive force of 25 cN.

From DSC curves, the values of the glass transition temperature, T_g, (as the midpoint of the change in heat capacity, c_p, in the glass transition region), the values of crystallization temperature, T_c, (the onset of the first crystallization peak) and the values of peak temperatures, T_p, (the maximum of the first crystallization peak) were evaluated. From the obtained thermodilatometric (TD) curves the coefficient of thermal expansion, α, was determined as a mean value in the temperature range of 150–250 °C, the glass transition temperature, T_g, was determined from the change in the slope of the elongation versus temperature plot and the dilatometric softening temperature, T_d, was obtained from the maximum of the expansion trace corresponding to the onset of viscous deformation. Evaluation of DSC and dilatometric curves was done by Proteus software (NETZSCH).

For the study of nucleation by DSC, 100 mg of the glass with the average particle size of $\sim$10 μm was first heated (10 °C min^{-1}) in DTA equipment from room temperature to a nucleation temperature, T_n (between T_g and T_c) and then nucleated at T_n for nucleation time, t_n, 30 min. After subsequent cooling to 100 °C, the sample was heated again to the temperature above the crystallization peak at a rate of 10 °C min^{-1}. This process was applied for several nucleation temperatures, T_n.

Heating microscopy thermal analysis was carried out using powder samples compacted to cylinders of 3 mm in diameter and about 3 mm in height by hand press. Analysis was performed on α-Al_2O_3 sample holder, with a heating rate of 5 °C min^{-1} from 400 to 1000 °C under static air atmosphere. The changes of the samples during sintering were estimated by evaluating the sample's projected area at different temperatures throughout the experiment. The projected area was observed by a video camera, and its changes were quantified using image analysing software. For each sample composition, three sintering experiments were carried out and the results were averaged.

Crystalline phases were identified by X-ray powder diffraction analysis using Cu Kα radiation on a Bruker D8 Advance diffractometer. Crystalline samples were prepared using isothermal heating of powdered glasses ($\sim$10 μm) at 560–780 °C (depending on composition) in a graphite mould for 2 h under an inert atmosphere (N_2).

Results and Discussion

By the procedure described above, 9 homogeneous glasses in the compositional series $(100 - x)[0.5ZnO–0.1B_2O_3–0.4P_2O_5]–xTeO_2$ with nominal TeO_2 contents between 0 and 80 mol% TeO_2 ($x = 0$; 10; 20; 30; 40; 50; 60; 70; 80) were prepared. The volatilisation losses were not significant, hence the batch compositions can be considered as reflecting actual compositions. A structureless XRD

spectrum was obtained for all glass compositions. The colour of the glasses varied from colourless ($x = 0$) through violet ($x = 10$) to brown ($x = 50$) and yellow ($x = 80$ mol% TeO_2) according to increasing TeO_2 content.

Results obtained from dilatometric curves are given in Fig. 1. It can be seen that incorporation of TeO_x structural units into the borophosphate glass network [19], results in an increase of thermal expansion coefficient, α, of glasses, while the glass transition temperature, T_g, and dilatometric softening temperature, T_d, steeply decrease (see Fig. 1). The values of α increase from 5.8 ($x = 0$ mol% TeO_2) to 12.2 ppm °C^{-1} ($x = 80$), while the values of T_g shift down from 459 °C ($x = 0$ mol% TeO_2) to 358 °C ($x = 80$) with the replacement of starting glass composition $50ZnO–10B_2O_3–40P_2O_5$ by TeO_2. The dilatation softening temperature, T_d, was higher by 20–44 °C than T_g values and differences between T_d and T_g decreases with increasing concentration of TeO_2 in the glasses (see Fig. 1). The observed changes, especially decrease in T_g and increase in α show the decreasing bonding strength in the glass structure with increasing TeO_2 content which is associated with the replacement of stronger P–O and B–O bonds by weaker Te–O bonds.

Structural studies [19] of these glasses by Raman, IR and ^{31}P MAS NMR spectroscopies showed that TeO_2 is incorporated in the structural network in the form of TeO_3, TeO_{3+1} and TeO_4 structural units. The ratio of TeO_4/TeO_3 increases with increasing TeO_2 content in the glasses. The incorporation of TeO_2 modifies also the coordination of boron atoms, where $B(OP)_4$ structural units are gradually replaced by $B(OP)_{4-n}(OTe)_n$ units [19].

DSC curves of studied glass series are shown in Fig. 2 and the values of glass transition temperature, T_g, crystallization temperature, T_c, and peak temperature, T_p, obtained from these curves are summarized in Table 1. Compositional trend of T_g values is similar to the trend in T_g determined from dilatometric curves (T_g values decrease with TeO_2 content), nevertheless from the TD curves lower values of T_g by 3–9 °C were determined than the T_g values obtained from DSC curves as the midpoint of ΔC_p in the glass transition region. The change of heat capacity, ΔC_p, in the glass transition region increases with increasing TeO_2 content, reveals a maximum at the glass containing 40 mol% TeO_2, having probably the highest fragility. DSC curves (Fig. 2) show also that most of glasses (solidified melts) crystallize on heating. The lowest tendencies towards crystallization have the glasses containing 50 and 60 mol% TeO_2. Thermoanalytical curves of glasses with a low TeO_2 content reveal at least two crystallization steps, as well as the glasses with a high TeO_2 content. The crystallization temperature, T_c, steeply decreases with increasing TeO_2 content from 636 °C (for $x = 0$) down to 443 °C for the glass containing 80 mol% TeO_2. A similar dependence on TeO_2 content has been observed for the peak temperature. Peak temperature, T_p, was higher by 9–34 °C than T_c values (see Table 1). The lowest difference between T_p and T_c values (the sharpest crystallization peak) was found for the glass containing 80 mol% TeO_2

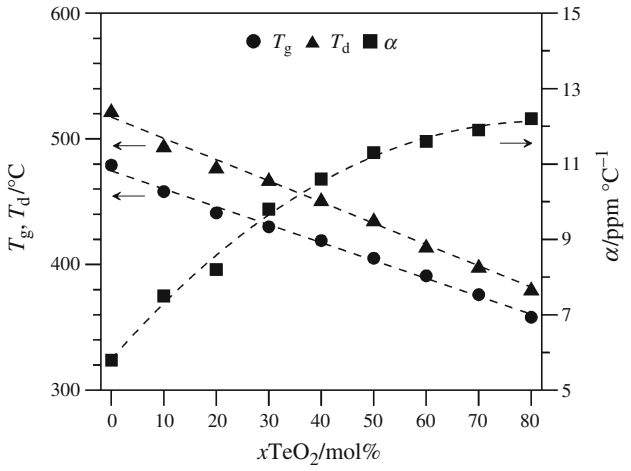

Fig. 1 Glass transition temperature, T_g, dilatation softening temperature, T_d and thermal expansion coefficient, α, of $(100 - x)[0.5ZnO–0.1B_2O_3–0.4P_2O_5]–xTeO_2$ glasses, obtained from thermodilatometric curves (the *lines* are only a guide to eye)

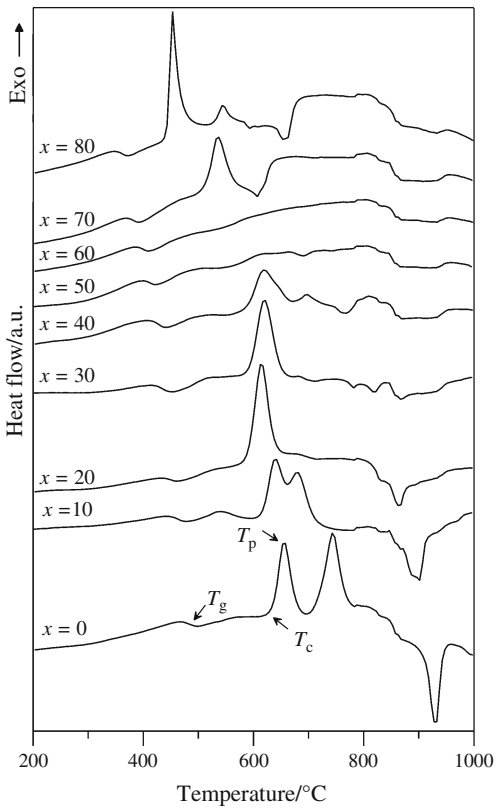

Fig. 2 DSC curves of $(100 - x)[0.5ZnO–0.1B_2O_3–0.4P_2O_5]–xTeO_2$ glasses

Table 1 Composition, glass transition temperature, T_g, crystallization temperature, T_c, peak temperature, T_p, flow temperature, T_f, criterion of glass stability, $T_c - T_g$, of $(100 - x)[0.5ZnO–0.1B_2O_3–0.4P_2O_5]–xTeO_2$ glasses and survey of crystalline products identified by XRD in the samples annealed at various temperatures for 2 h

ZnO/ mol%	B_2O_3/ mol%	P_2O_5/ mol%	TeO_2/ mol%	$T_g \pm 2$*/°C	$T_c \pm 2$/°C	$T_p \pm 1$/°C	$T_f \pm 3$/°C	$T_c - T_g$*/°C	Crystalline products
50	10	40	0	482	636	656	901	154	$Zn_2P_2O_7 + BPO_4$/780 °C
45	9	36	10	466	617	640	876	151	$Zn_2P_2O_7 + BPO_4$/750 °C
40	8	32	20	450	590	614	832	140	$Zn_2P_2O_7 + BPO_4$/720 °C
35	7	28	30	437	594	620	789	157	$Zn_2P_2O_7 + BPO_4 + \alpha$-$TeO_2$/720 °C
30	6	24	40	425	586	620	727	161	$Zn_2P_2O_7 + BPO_4 + \alpha$-$TeO_2$ + glass/720 °C
25	5	20	50	413	–	–	626	–	Glass/550, 600, 650 °C
20	4	16	60	400	–	–	584	–	Glass/550, 600, 650 °C
15	3	12	70	382	513	535	591	131	α-TeO_2/560 °C
10	2	8	80	361	443	452	624	82	α-TeO_2/560 °C

* T_g values obtained from DSC curves

(see Fig. 2). The melting temperature could not be evaluated from DSC curves due to reaction of the silica crucibles with melt (see Fig. 2). Instead of the melting temperature a flow temperature, T_f, was evaluated from temperature curve obtained by heating microscopy. The flow temperature was obtained as the first temperature at which the height of the melted test piece was one-third of its original height at the start of the measurement. As can be seen in Table 1, T_f values steeply decrease with increasing TeO_2 content having a minimum at $x = 60$ mol% TeO_2. The increase in T_f values for the glasses containing more than 60 mol% TeO_2 can be related to a lower thermal stability and higher degree of crystallinity under experimental conditions which have been used for the measurements. Thermal stability of glasses was evaluated from the difference of $T_c - T_g(\Delta T)$, where higher values of ΔT correspond to a higher thermal stability. For these calculations, T_g values obtained from DSC measurements were used and the obtained values of $T_c - T_g$ difference are given in Table 1. We can see that thermal stability, evaluated by ΔT criterion, exhibits two maxima. Relatively high thermal stability has the parent $50ZnO–10B_2O_3–40P_2O_5$ borophosphate glass; nevertheless with addition of TeO_2 thermal stability gradually decreased having a minimum at $x = 20$ mol% TeO_2. The highest thermal stability and therefore the lowest tendency towards crystallization revealed glasses containing 50 and 60 mol% TeO_2 as on their DSC curves crystallization peak was not observed. On the other hand, the lowest thermal stability was found for the glasses containing the highest TeO_2 content (see Table 1).

XRD patterns of the samples crystallized for 2 h at the temperatures between 560 °C ($x = 80$) and 780 °C ($x = 0$ mol% TeO_2) are shown in Fig. 3. The X-ray diffraction analysis showed that by heating the parent zinc borophosphate glass at 780 °C, crystalline zinc diphosphate $Zn_2P_2O_7$ phase and crystalline boron phosphate BPO_4 phase were formed. With increasing TeO_2 content, diffraction lines of crystalline $Zn_2P_2O_7$ and BPO_4 phases are gradually replaced by more intensive diffraction lines of α-TeO_2 (paratellurite) phase [20, 21]. Similar crystalline phases were formed also by calcination of starting mixture for 2 h at 600 °C, nevertheless in some sample compositions we have observed in X-ray diffraction patterns also

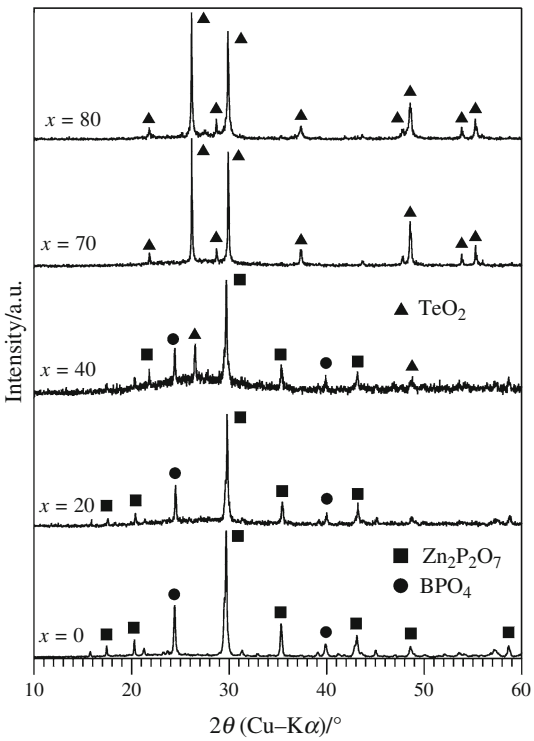

Fig. 3 XRD patterns of $(100 - x)[0.5ZnO–0.1B_2O_3–0.4P_2O_5]–xTeO_2$ powdered glasses annealed at 530–775 °C for 2 h

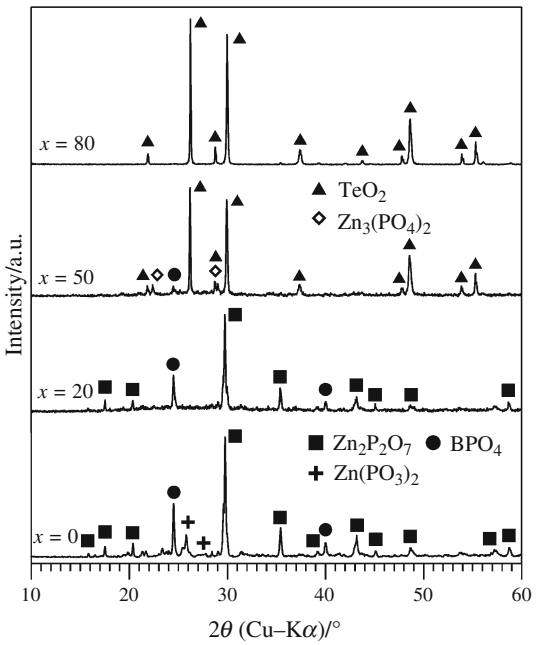

Fig. 4 XRD patterns of the $(100 - x)[0.5ZnO–0.1B_2O_3–0.4P_2O_5]–xTeO_2$ starting mixtures calcined at 500 °C for 2 h

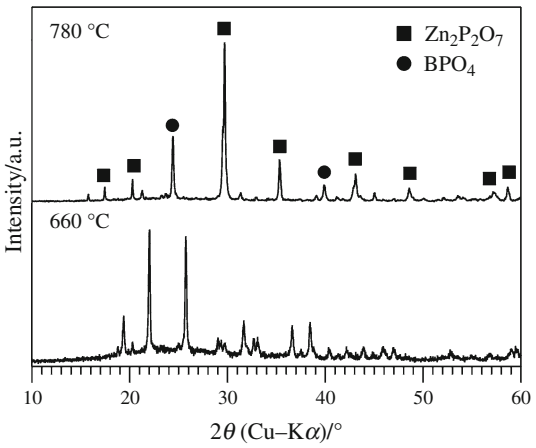

Fig. 5 XRD patterns of the $50ZnO–10B_2O_3–40P_2O_5$ powdered glass annealed up to 660 and 775 °C

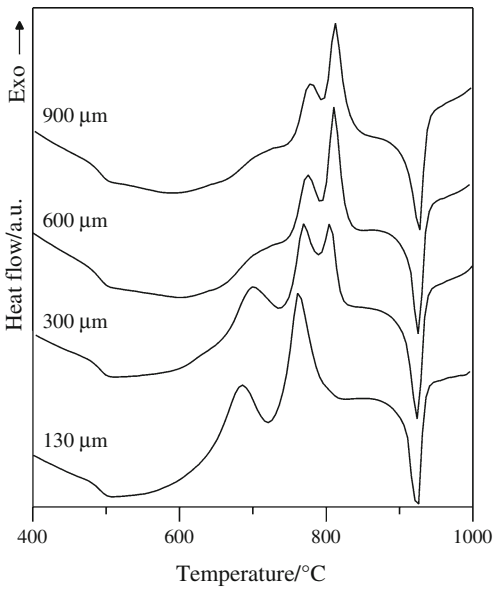

Fig. 6 DSC curves of the $50ZnO–10B_2O_3–40P_2O_5$ glass as function of particle size

diffraction lines of $Zn(PO_3)_2$ ($x = 0$) and $Zn_3(PO_4)_2$ ($x = 50$ mol% TeO_2; see Fig. 4). Small amounts of $Zn(PO_3)_2$ and $Zn_3(PO_4)_2$ compounds in the calcined starting mixture can be related to some inhomogeneity of the starting mixture. The X-ray diffraction analysis also showed that long-run isothermal heating of glasses containing 50 and 60 mol% TeO_2 at various temperatures (550, 600 and 650 °C) did not lead to the crystallization. Degree of crystallinity was checked also by Raman spectroscopy. Raman spectra showed that also glass containing 40 mol% TeO_2 has a relatively high thermal stability, and its annealing leads only to the partial crystallization (see Table 1). In the parent glass of the composition $50ZnO–10B_2O_3–40P_2O_5$, we also found that the first crystallization peak corresponds to the formation of unknown, probably borophoshate crystalline phase, which was gradually transformed to $Zn_2P_2O_7$ and BPO_4 during subsequent heating (see Fig. 5).

From the DSC curves obtained at the heating rate of 10 °C min^{-1} for different particle sizes (120, 300, 600 and 900 µm; see Fig. 6), it is evident that with increasing particle size, the first crystallization peak corresponding to the formation of an unknown phase becomes weaker and the second crystallization peak is decomposed into two individual peaks reflecting the formation of BPO_4 (first crystallization peak) and $Zn_2P_2O_7$ (second peak). These results suggest that the unknown phase nucleates predominantly by a surface crystallization mechanism and that the contribution of the volume/surface crystallization mechanism during the formation of BPO_4 and $Zn_2P_2O_7$ is different.

DSC curves that were obtained after 30 min heat treatments of the starting glass composition $50ZnO–10B_2O_3–40P_2O_5$ (particle size ~10 µm) at various nucleation temperatures, T_n, (from 500 to 680 °C) are shown in Fig. 7. As we can see in this figure, the starting zinc borophospate glass exhibits relatively high thermal stability. During 30 min isothermal annealing at the nucleation temperature, T_n, from 500 to 590 °C, i.e., from ~20 to 110 °C above the glass transition temperature only very small amount of stable nuclei is formed, which is evident from the changes of the crystallization peaks height. The most substantial changes of the crystallization peaks height and nucleation rate were observed at the nucleation temperature above 590 °C (see Fig. 7), when the first crystallization peak corresponding to

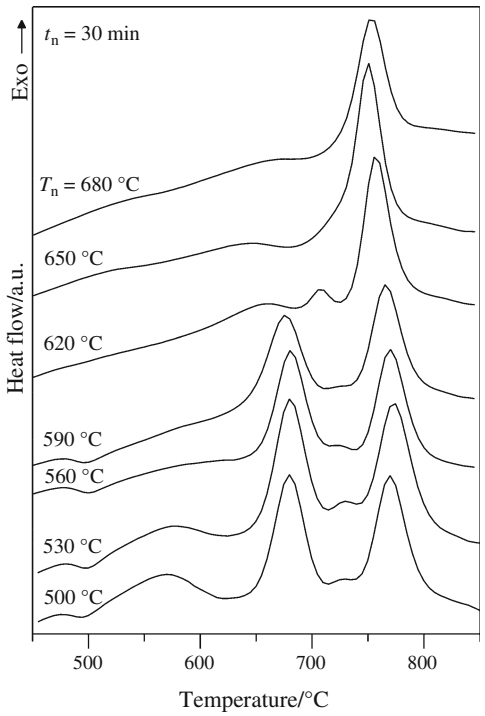

Fig. 7 DSC curves of the $50ZnO–10B_2O_3–40P_2O_5$ glass as function of nucleation temperature, T_n, for 30 min

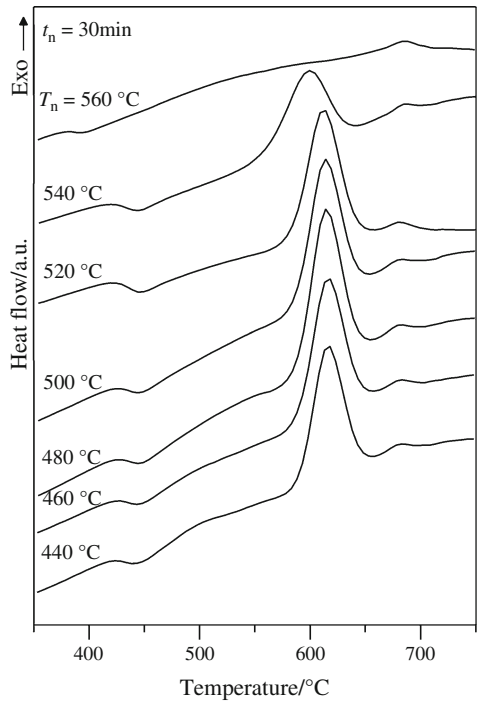

Fig. 8 DSC curves of the $70[0.5ZnO–0.1B_2O_3–0.4P_2O_5]–30TeO_2$ glass as function of nucleation temperature, T_n, for 30 min

the formation of unknown phase from the DSC curve practically disappears. For the sample nucleated 30 min at 620 °C (close to T_c; see Table 1) only second crystallization peak was observed in the DSC curves, indicating formation of both BPO_4 and $Zn_2P_2O_7$ phases. The same DSC measurements were applied for the study of nucleation of the $70[0.5ZnO–0.1B_2O_3–0.4P_2O_5]–30TeO_2$ glass. DSC curves obtained by continuous heating of this glass after previous 30 min heat treatments at nucleation temperatures, T_n, from 440 to 560 °C are shown in Fig. 8. From this figure it is evident, that this powdered glass containing 30 mol% of TeO_2 is saturated with a substantial amount of stable nuclei at the nucleation temperature above 500 °C (i.e. ~60 °C above T_g). On the other hand, at nucleation temperatures close to 560 °C, the nucleation rate is too small to produce any additional nuclei and crystallization peak from the DSC curve practically disappears.

Conclusions

The study of $(100 - x)[0.5ZnO–0.1B_2O_3–0.4P_2O_5]–xTeO_2$ glasses revealed that replacement of starting zinc borophosphate composition by TeO_2 leads to significant changes in the thermal properties of these glasses. DSC and TD measurements showed that the incorporation of TeO_2 into the borophosphate structural network and gradual replacement of stronger P–O and B–O bonds by weaker Te–O bonds results in a decrease of the glass transition temperature and the dilatometric softening temperature, while thermal expansion coefficient of the glasses decreases. Gradual transformation of the borophospate network structure to the structure predominantly composed of TeO_x units results also in a significant decrease of crystallization temperature, nevertheless, thermal stability of glasses increases having a maximum at $x = 50$ and 60 mol% TeO_2. Raman spectra showed that also glass containing 40 mol% TeO_2 have a relatively high thermal stability and its annealing leads only to the partial crystallization. Residual glassy matrix of this sample consists mainly of vitreous TeO_2. Study of nucleation rate of the glasses containing 0 and 30 mol% TeO_2 indicated that annealing of their powdered solidified melts leads to the fully crystalline samples. Nevertheless, the samples are saturated with a substantial amount of stable nuclei at relatively high temperatures above T_g.

Acknowledgements The authors are grateful for the financial support from the research project No. 0021627501 of the Ministry of Education of Czech Republic and from the Grant Agency of the Czech Republic (Grant No. P106/10/0283).

References

1. Takebe H, Baba Y, Kuwabara M. Dissolution behavior of ZnO–P_2O_5 glasses in water. J Non-Cryst Solids. 2006;352:3088–94.

2. Donald IW, Metcalfe BL, Bradley DJ, Hill MJC, McGrath JL, Bye AD. The preparation and properties of some lithium borate based glasses. J Mater Sci. 1994;29:6379–96.
3. Koudelka L, Mošner P. Study of the structure and properties of Pb-Zn borophosphate glasses. J Non-Cryst Solids. 2001;293–295: 635–41.
4. Lim JW, Schmitt ML, Brow RK, Yung SW. Properties and structures of tin borophosphate glasses. J Non-Cryst Solids. 2010; 356:1379–84.
5. Szumera M, Waclawska I, Olejniczak Z. Influence of B_2O_3 on the structure and crystallization of soil active glasses. J Therm Anal Calorim. 2010;99:879–86.
6. Baikova LG, Fedorov YK, Pukh VP, Tikhonova LV, Kazannikova TP, Sinani AB, Nikitina SI. Influence of boron oxide on the physicomechanical properties of glasses in the $Li_2O–B_2O_3–P_2O_5$ system. Glass Phys Chem. 2003;29:276–81.
7. Liu SJ, Lu AX, Tang XD, He SB. Influence of addition of B_2O_3 on properties of Yb^{3+}-doped phosphate laser glass. J Cent South Univ Technol. 2006;13:468–72.
8. Muñoz F, Montagne L, Pascual L, Durán A. Composition and structure dependence of the properties of lithium borophosphate glasses showing boron anomaly. J Non-Cryst Solids. 2009;355: 2571–7.
9. Mošner P, Koudelka L. Glass-forming ability, thermal stability and chemical durability of lead borophosphate glasses. Phosphorus Res Bull. 2002;13:197–200.
10. Saranti A, Koutselas I, Karakassides MA. Bioactive glasses in the system $CaO–B_2O_3–P_2O_5$: preparation, structural study and in vitro evaluation. J Non-Cryst Solids. 2006;352:390–8.
11. Kumar S, Vinatier P, Levasseur A, Rao KJ. Investigations of structure and transport in lithium and silver borophosphate glasses. J Solid State Chem. 2004;177:1723–37.
12. Ushakov DF, Baskova NF, Tarlakov YP. Glass formation in the zinc oxide-boron oxide (B_2O_3)-phosphorus pentoxide system. Fiz Khim Stekla. 1975;1:151–6.
13. Brow RK. An XPS study of oxygen bonding in zinc phosphate and zinc borophosphate glasses. J Non-Cryst Solids. 1996;194: 267–73.
14. Brow RK, Tallant DR. Structural design of sealing glasses. J Non-Cryst Solids. 1997;222:396–406.
15. Koudelka L, Mošner P. Borophosphate glasses of the $ZnO-B_2O_3–P_2O_5$ system. Mater Lett. 2000;42:194–9.
16. Mošner P, Koudelka L. Kinetics and mechanism of crystallization of borophosphate glasses of the $ZnO-B_2O_3–P_2O_5$ system. Sci Pap Univ Pardubice Ser A. 1998;4:75–85.
17. Khafagy AH, El-Adawy AA, Higazy AA, El-Rabaie S, Eid AS. The glass transition temperature and infrared absorption spectra of: $(70 - x)TeO_2 + 15B_2O_3 + 15P_2O_5 + xLi_2O$ glasses. J Non-Cryst Solids. 2008;354:1460–6.
18. Khafagy AH, El-Adawy AA, Higazy AA, El-Rabaie S, Eid AS. Studies of some mechanical and optical properties of: $(70 - x)$ $TeO_2 + 15B_2O_3 + 15P_2O_5 + xLi_2O$ glasses. J Non-Cryst Solids. 2008;354:3152–8.
19. Mošner M, Vosejpková K, Koudelka L, Montagne L, Revel B. Structure and properties of $ZnO-B_2O_3-P_2O_5-TeO_2$ glasses. Mater Chem Phys. 2010;124:732–7.
20. Araújo EB, Idalgo E. Non-isothermal studies on crystallization kinetics of tellurite $20Li_2O–80TeO_2$ glass. J Therm Anal Calorim. 2009;95:37–42.
21. Sidel SM, Santos FA, Gordo VO, Idalgo E, Monteiro AA, Moraes JCS, Yukimitu K. Avrami exponent of crystallization in tellurite glasses. J Therm Anal Calorim. 2011. doi 10.1007/s10973-011-1312-4.